SPANDIDOS PUBLICATIONS

ONCOLOGY LETTERS 28: 425, 2024

Cancer marker TNFRSF1A: From single-cell heterogeneity of renal cell carcinoma to functional validation

PING XU*, ZUSHENG DU*, XIAOHONG XIE, LIFEI YANG and JINGJING ZHANG

Department of Ultrasound, Ningbo Yinzhou No. 2 Hospital, Ningbo, Zhejiang 315153, P.R. China

Received January 15, 2024; Accepted June 6, 2024

DOI: 10.3892/ol.2024.14559

Abstract. During the progression of renal cell carcinoma (RCC), tumor growth, metastasis and treatment response heterogeneity are regulated by both the tumor itself and the tumor microenvironment (TME). The aim of the present study was to investigate the role of the TME in RCC and construct a crosstalk network for clear cell RCC (ccRCC). An additional aim was to evaluate whether TNF receptor superfamily member 1A (TNFRSF1A) is a potential therapeutic target for ccRCC. Single-cell data analysis of RCC was performed using the GSE152938 dataset, focusing on key cellular components and their involvement in the ccRCC TME. Additionally, cell-cell communication was analyzed to elucidate the complex network of the ccRCC microenvironment. Analyses of data from The Cancer Genome Atlas and Clinical Proteomic Tumor Analysis Consortium databases were performed to further mine the key TNF receptor genes, with a particular focus on the prediction and assessment of the cancer-associated features of TNFRSF1A. In addition, following the silencing of TNFRSF1A using small interfering RNA in the 786-O ccRCC cell line, a number of *in vitro* experiments were conducted to further investigate the cancer-promoting characteristics of TNFRSF1A. These included 5-ethynyl-2'-deoxyuridine incorporation, Cell Counting Kit-8, colony formation, Transwell, cell cycle and apoptosis assays. The TNF signaling pathway was found to have a critical role in the development of ccRCC. Based on the specific crosstalk identified between TNF and TNFRSF1A, the communication of this signaling pathway within the TME was elucidated. The results of the cellular phenotype experiments indicated that TNFRSF1A promotes the proliferation, migration and invasion of ccRCC cells. Consequently, it is proposed that targeting TNFRSF1A may disrupt tumor progression and serve as a therapeutic strategy. In conclusion, by understanding the TME and identifying significant crosstalk within the TNF signaling pathway, the potential of TNFRSF1A as a therapeutic target is highlighted. This may facilitate an advance in precision medicine and improve the prognosis for patients with RCC.

Correspondence to: Dr Lifei Yang or Dr Jingjing Zhang, Department of Ultrasound, Ningbo Yinzhou No. 2 Hospital, 998 Qianhe Road, Yinzhou, Ningbo, Zhejiang 315153, P.R. China
E-mail: 1399330109@qq.com
E-mail: sally4381@163.com

*Contributed equally

Key words: tumor microenvironment, renal cell carcinoma, TNFRSF1A, clear cell renal carcinoma, therapeutic target

Introduction

Kidney cancer, including its most frequently occurring type renal cell carcinoma (RCC), is a significant global health issue (1). With a mortality rate of ~175,000 death/year, kidney cancer markedly contributes to global cancer-related fatalities (2). RCC is a heterogeneous disease with various histological subtypes (3), including clear cell, papillary, chromophobe and collecting duct carcinoma. Clear cell RCC (ccRCC) is the most common histological subtype, comprising 70-80% of all kidney cancer cases (4). The prognosis and treatment options for kidney cancer depend on the stage of the disease at diagnosis, with advanced or metastatic cases presenting significant challenges for effective treatment (5).

The diagnosis of kidney cancer typically involves a combination of clinical evaluation, imaging techniques such as computed tomography scans and magnetic resonance imaging, and the pathological examination of tumor tissue obtained by biopsy or surgery (6,7). These diagnostic approaches may be used to determine the extent of tumor growth, invasion and metastasis, providing crucial information for the planning of treatment and assessment of prognosis.

Current treatment strategies for kidney cancer involve a multidisciplinary approach (7), including surgery, targeted therapies, immunotherapies and radiation therapy. Surgical intervention, such as partial or radical nephrectomy, remains the primary treatment option for localized kidney tumors (6). However, the management of advanced or metastatic kidney cancer poses considerable challenges, as it is often associated with a poor prognosis and limited treatment options (8).

Substantial progress has been made in understanding the molecular landscape of kidney cancer, leading to the development of targeted therapies (5,9). Agents that inhibit the vascular endothelial growth factor (VEGF) pathway, such as tyrosine kinase inhibitors (TKIs) (10) and anti-angiogenic monoclonal antibodies (11), have shown efficacy in the treatment of advanced kidney cancer. In addition, immune

checkpoint inhibitors targeting programmed cell death protein 1 (PD-1) and PD-ligand 1 have demonstrated marked clinical responses, highlighting the importance of the immune system in combating kidney cancer (12,13).

Despite these advancements, treatment resistance and disease progression remain major obstacles in the management of kidney cancer. Therefore, it is urgently necessary to identify novel therapeutic targets and develop innovative treatment strategies for kidney cancer. Targeting tumor necrosis factor (TNF), a pro-inflammatory cytokine with complex roles in inflammation and immune regulation, has emerged as a potential therapeutic approach (14,15). A previous study indicated that TNF receptor superfamily member 1A (TNFRSF1A) and 1B (TNFRSF1B) are regulated under inflammatory conditions, with the former promoting inflammatory responses upon binding to TNF-α (16). However, whether TNFRSF1A is a pro-inflammatory factor that acts against cancer or aids in the immune evasion of cancer to promote carcinogenesis within renal cancer tissue remains to be validated and explored.

In the present study, single-cell data analysis of RCC was conducted to investigate the global characteristics of the tumor microenvironment. The aim was to analyze the roles played by key cellular components in the tumor microenvironment and predict the involvement of the TNF signaling pathway in the development of ccRCC. Comprehensive analysis suggested that TNFRSF1A may play a pivotal role in the progression of ccRCC. Therefore, cell experiments assessing proliferation, migration, invasion, the cell cycle and apoptosis were performed to validate the pro-cancer effects of TNFRSF1A and its potential as a therapeutic target for ccRCC. Ultimately, the goal of the present study was to contribute to the advancement of precision medicine and improve the prognosis for patients with kidney cancer.

Materials and methods

Data sources. The raw single-cell sequencing data of 4 cases of RCC and 1 case of normal kidney tissue were obtained from the dataset GSE152938 (17) in the Gene Expression Omnibus (https://www.ncbi.nlm.nih.gov/gds) database. Additionally, the sequencing data and clinical information of patients with ccRCC were obtained from The Cancer Genome Atlas (TCGA; https://portal.gdc.cancer.gov) database.

Single-cell data download and conversion. Under the Linux environment, the Sequence Read Archive (SRA) Toolkit version 2.11.3 (https://github.com/ncbi/sra-tools) was used as follows: i) The prefetch tool was utilized to download the sample data in the original SRA data format. ii) as the dataset was generated using paired-end sequencing, the dump tool was employed to split and convert the SRA files into 2-3 FASTQ files, with each SRA file yielding two FASTQ files due to the high sequencing quality of the dataset; and iii) files were renamed for improved data organization and management.

scRNA-fseq data preprocessing

Sequence quality control and alignment. FastQC (version 0.11.7; available at: http://www.bioinformatics.babraham.ac.uk/projects/fastqc/) was executed in a Linux environment to perform a quality control assessment of each FASTQ file. Cellranger (version 6.1.2; https://www.10xgenomics.com/support/software/cell-ranger/) was then utilized for data alignment using the reference genome refdata-gex-GRCh38-2020-A. The cellranger count command was used to align the sequencing files with the reference genome, resulting in matrix.mtx.gz, features.tsv.gz and barcodes.tsv.gz files that were used for downstream bioinformatics analysis.

Preprocessing for analysis. The processed data were loaded into Seurat (version 3.1.1; https://github.com/satijalab/seurat/) for single-cell analysis. Initially, the scDblFinder (version 3.16; https://github.com/plger/scDblFinder) package was used to filter doublet cells from the dataset. Additionally, genes associated with ribosomes, mitochondria and blood cells were removed to eliminate interference. The filtering and quality control criteria were set as follows: Genes expressed in ≥1 cell, cells expressing ≥700 genes, count value ≥600 for each gene, unique molecular identifier counts <500 and mitochondrial gene expression limited to ~15% of total gene expression in each single cell.

Cell type and subtype identification. Seurat v3.1.1 were applied to integrate the single-cell data from 18,347 ccRCC cells, 3,365 normal kidney tissue cells, 10,168 papillary RCC cells, and 8,216 chromophobe RCC cells. SCTransform (version 0.3.5; https://github.com/satijalab/sctransform) was used for further data normalization and the calculation of expression values. Principal component analysis (PCA) and non-linear dimensionality reduction were performed using the normalized expression values. Subsequently, preliminary clustering results were visualized using t-distributed stochastic neighbor embedding (t-SNE) and uniform manifold approximation and projection (UMAP) algorithms. PCA, t-SNE and UMAP were performed using Seurat v3.1.1. Cell identification was performed using the SingleR (version 1.0; https://github.com/dviraran/SingleR) package with manual identification based on marker genes, resulting in several cell clusters and their corresponding cell types. Further subclustering was performed using the same methods to identify cell subtypes.

Copy number variation (CNV) analysis. The infercnv (version 1.16.0; https://github.com/broadinstitute/infercnv) package was used to determine large-scale chromosomal CNVs in somatic cells based on single-cell data. This package inferred chromosomal variations by comparing the expression intensity of genes at different positions in tumor RNA to that in a set of reference normal cells.

Functional annotation and pathway enrichment. Gene Ontology (GO) functional annotation and Kyoto Encyclopedia of Genes and Genomes (KEGG) pathway enrichment analyses were conducted using the GO (https://www.geneontology.org/) and KEGG (https://www.genome.jp/kegg/) databases to elucidate the higher-level functions and roles of relevant genes and proteins in biological systems. GO terms and KEGG pathways with a Q-value ≤0.05 were considered significantly enriched. Both tools were implemented using the R programming language. Abnormal cell signaling can cause cancer and is a common target for treatment. The PROGENy (version 1.22.0; https://saezlab.github.io/progeny/) package was used to infer the signaling pathway activity of 14 abnormal

signaling pathways based on the gene expression data from the present study, namely androgens, estrogens, EGFR, hypoxia, JAK-STAT, MAPK, NF-κB, PI3K, p53, TGF-β, TNF-α, Trail, VEGF and WNT.

Pseudotime computation. Pseudotime analysis is a method used to infer the developmental trajectory of cells (18). It is based on single-cell transcriptomic data and involves quantifying the similarity of cells, grouping the cells and arranging them in a sequence that reflects their development and reveals their sequential progression. The Monocle (version 2.26.0; http://cole-trapnell-lab.github.io/monocle-release/) package was utilized to perform a single-cell trajectory analysis, employing the DDR-Tree algorithm. In addition, the Slingshot (version 2.8.0) package (19) was used to infer the lineage of cells as they differentiate, structure the lineages and place them on the original visualized clustered graph.

Cell communication. Cell-cell communication (20) mediated by ligand-receptor complexes plays a crucial role in tumor development and the associated inflammatory responses. The iTALK (https://github.com/Coolgenome/iTALK) package was used to compare the expression of ligand and receptor genes between different cell types in RCC tissues, and thereby reveal intercellular communication interactions. iTALK performs analyses based on ligand-receptor expression patterns, co-expression analysis and pathway enrichment analysis to elucidate cell-cell communication networks. Additionally, the CellChat package (version 1.4.0; http://www.cellchat.org) (21) was used to further analyze and visualize cell-cell communication networks for continuous cell states along their developmental trajectories. These two tools were integrated to perform a comprehensive analysis of single-cell RNA sequencing data, and elucidate complex cell-cell communication networks within the ccRCC microenvironment. The ggalluvial package (https://corybrunson.github.io/ggalluvial) was used to visualize the cell-cell networks into riverplots.

Bioinformatics analysis. The sequencing data and clinical information of patients with ccRCC were downloaded from TCGA database for gene expression analysis and the statistical analysis of clinical data. The protein expression levels of genes positively associated with TNFRSF1A and TNFRSF1B were derived from protein expression data for ccRCC and normal tissues from the Clinical Proteomic Tumor Analysis Consortium (CPTAC), which were accessed via the UALCAN online database (22).

Cell culture. The human kidney carcinoma cell line 786-O and human renal proximal tubular epithelial cell line HK-2 were bought from Shanghai Zhongqiao Xinzhou Biotechnology Co., Ltd. The 786-O cells were cultured in RPMI-1640 (HyClone; Cytiva) and the HK-2 cells were cultured in DMEM (HyClone; Cytiva); both were supplemented with 10% heat-inactivated FBS (PAN-Biotech GmbH) and 1% Penicillin-Streptomycin (Gibco; Thermo Fisher Scientific, Inc.) in a 5% CO_2 incubator at 37°C.

Transfection of TNFRSF1A small interfering RNA (siRNA) into 786-O cells. TNFRSF1A siRNA (si-TNFRSF1A) was used to suppress TNFRSF1A expression in the experimental group. The sequences of si-TNFRSF1A were as follows: Sense, 5'-GUGGAGAUCUCUUCUUGCATT-3' and antisense, 5'-UGCAAGAAGAGAUCUCCACTT-3'. A non-silencing siRNA negative control (si-NC) was used to establish the NC group. The sequences of si-NC were as follows: Sense, 5'-UUC UCCGAACGUGUCACGUTT-3' and antisense, 5'-ACG UGACACGUUCGGAGAATT-3' (Shanghai GenePharma Co., Ltd.). Lipofectamine® 2000 (Invitrogen; Thermo Fisher Scientific. Inc.) was used as the transfection reagent. The cells were transfected at 37°C for 2 h with 20 pM siRNA in a 1:1 volume with Lipofectamine 2000, after which, the medium was replaced with complete medium. After a further 24 h of incubation at 37°C, the cells were used in further experiments.

Reverse transcription-quantitative polymerase chain reaction (RT-qPCR). Total RNA was extracted from the cells using TRIzol® reagent (Invitrogen; Thermo Fisher Scientific. Inc.). RT was carried out using a RT kit (Promega GoScript™ Reverse Transcription System; Thermo Fisher Scientific. Inc.), according to manufacturer's protocol, and qPCR was then performed using SYBR Green methodology (PerfectStart® Green qPCR SuperMix; TransGen Biotech Co., Ltd.). The thermal cycling conditions for qPCR were as follows: Initial denaturation at 94°C for 5 min, followed by 40 cycles of denaturation at 94°C for 15 sec and annealing/extension at 60°C for 1 min. GAPDH was the internal reference gene. The primer sequences (BGI Genomics) were as follows: TNFRSF1A forward, 5'-ATTGGACTGGTCCCTCACCT-3'- and reverse, 5'-CACTCCCTGCAGTCCGTATC-3'; GAPDH forward, 5'-AAGGTGAAGGTCGGAGTCAA-3' and reverse, 5'-AAT GAAGGGGTCATTGATGG-3'. The $2^{-\Delta\Delta Cq}$ method was used for quantification (23). The silencing effect of si-TNFRSF1A was confirmed by RT-qPCR. The expression levels in the si-TNFRSF1A group were compared with those in the NC and mock groups using one-way ANOVA followed by Tukey's honestly significant difference (HSD) post hoc tests.

Cell proliferation. Cell Counting Kit-8 (CCK-8; Dojindo Laboratories, Inc.) was used to assess the proliferation of 786-O cells. Specifically, $5x10^3$ cells in 100 μl were seeded per well of a 96-well plate 24 h after transfection. Each treatment group was subjected to testing with ≥3 replicates. Cell proliferation was detected at 0, 24, 48 and 72 h after seeding. The cells were incubated with the CCK-8 reagent for 2 h and the absorbance of each sample was determined at 450 nm using a microplate reader (SpectraMax M5; Molecular Devices, LLC).

A 5-ethynyl-2'-deoxyuridine (EdU) assay was also performed, in which 786-O cells 24 h after siRNA transfection were treated with 10 μM EdU for 2 h using the BeyoClick™ EdU Cell Proliferation Kit with Alexa Fluor 594 (Beyotime Institute of Biotechnology). Subsequently, the cells were fixed with 4% polyformaldehyde in PBS at room temperature for 30 min, washed and then incubated with Enhanced Immunostaining Permeabilization Solution (Beyotime Institute of Biotechnology) at room temperature for 10 min. After additional washes, the cells were incubated with Click Addictive Solution (Beyotime Institute of Biotechnology) for 30 min in the dark at room temperature. Finally, the cell nuclei were stained with 1X Hoechst 33343

solution at room temperature for 10 min. Fluorescence microscopy was performed in five randomly selected fields to assess the proliferation rate. Blue fluorescence represented Hoechst 33343 staining of the cell nuclei, red fluorescence indicated the staining of EdU in proliferating cells, and the red/blue ratio indicated the proportion of proliferating cells. All assays were repeated at least three times.

Colony formation assay. A single cell suspension comprising 786-O cells treated with either si-TNFRSF1A or si-NC was prepared. The suspension was diluted to $1x10^3$ cells/well in a 6-well plate with three replicates per group, and then 2 ml RPMI-1640 was added. The plates were incubated in a humidified atmosphere at 37˚C with 5% CO_2 for 2 weeks. Images were captured after 30-min fixing with 4% paraformaldehyde and 10-min staining with 0.1% crystal violet at room temperature. The number of cell colonies was manually counted. Each independently counted colony refers to a cluster of ≥50 cells visible under the microscope, with clear boundaries or spatial separation from other colonies. The experiment was repeated three times.

Cell migration and invasion assays. For the wound healing assay, the transfected 786-O cells were seeded in 6-well plates and cultured until they reached 80-90% confluence. Next, a straight line was scratched in the middle of the cell layer in each well with a 2-ml pipette tip and the RPMI-1640 medium was replaced with Opti-MEM I Reduced Serum Medium (Gibco; Thermo Fisher Scientific, Inc.) The wounds were imaged under an inverted fluorescence microscope (Nikon Corporation) at 0 and 24 h after wounding. The percentage reduction in the width of the wound after cell migration from the edge of the scratch to the center of the scratch was observed.

In the Transwell assays, $5x10^5$ cells/ml (100 μl) in Opti-MEM I Reduced Serum Medium were seeded in the upper chamber of a 24-well Transwell apparatus (Costar; Corning, Inc.), which contained either an uncoated or Matrigel-coated membrane. For pre-coating, the chambers were incubated with 10% Matrigel at 37˚C for 2 h. Then, 600 μl medium containing 20% FBS was placed the lower chambers. After 24 h at 37˚C, the cells that crossed the inserts were stained with 0.1% crystal violet at room temperature for 20 min and then washed with PBS. Finally, three fields in each well were randomly selected and images captured under a TS2FL inverted fluorescence microscope (Nikon Corporation) to count the number of migrated or invaded cells. In addition, the crystal violet was washed away with 200 μl 33% acetic acid, collected in a 96-well plate, and its absorption at 570 nm was measured. These experiments were repeated at least three times.

Cell cycle and apoptosis assays. For flow cytometric cell cycle analysis, following transfection with si-TNFRSF1A or si-NC for 24 h, 786-O cells were harvested and resuspended in 1 ml PBS ($1x10^6$/ml), and then treated according to the instructions of the Cell Cycle Staining Kit [MultiSciences (Lianke) Biotech Co., Ltd.]. Briefly, the supernatant was removed after centrifugation at 1,000 x g under room temperature for 3 min, then 1 ml DNA staining solution was added, and the cells were stained for 30 min in the dark at room temperature. Finally, the cell cycle was analyzed by flow cytometry (Beckman CytoFLEX S; Beckman Coulter, Inc.) using FlowJo software (version 10.9.0; FlowJo LLC) for quantification.

An Annexin V-FITC/PI staining assay was also performed to quantify apoptosis. Following transfection with si-TNFRSF1A or si-NC for 24 h, 786-O cells were collected, washed with PBS, and resuspended in 500 μl binding buffer. Subsequently, a mixture of 5 μl Annexin V-FITC and 10 μl PI [Annexin V-FITC/PI Apoptosis Kit; MultiSciences (Lianke) Biotech Co., Ltd.] was added to the cells, and the solution was incubated at room temperature for 5 min. The apoptotic cells were detected by flow cytometry and quantified using FlowJo v10.9.0 software. All samples were assayed in triplicate.

Statistical analysis. All data were processed using R software (version 3.6.0, https://cran-archive.r-project.org/bin/windows/base/old/3.6.0), GraphPad 8.0 (Dotmatics) and SPSS version 23.0 (IBM Corp.). Differences between two groups, including those in expression data from TCGA database, were examined using the unpaired t-test. Clinical data were analyzed using one-way ANOVA, as well as univariate and multivariate logistic regression analyses. One-way ANOVA was also used for the comparison of the three groups in the transfection assay. Tukey's HSD test was employed as the post hoc test following ANOVA. The stats package (version 4.3.2; https://www.rdocumentation.org/packages/stats/) was used to calculate the Pearson correlation coefficient, and the ggplot2 package (version 3.3.4; https://cran.r-project.org/src/contrib/Archive/ggplot2/) was used to visualize the results. RStudio (version 2023.06.0; https://docs.posit.co/ide/news/#rstudio-2023.06.0) was employed as the tool for analysis. Data are presented as the mean ± standard deviation. $P<0.05$ was considered to indicate a statistically significant result. All experiments were performed at least three times.

Results

Single-cell landscape and phenotypes of RCC. Raw data obtained for RCC and normal kidney tissues were preprocessed to obtain the corresponding expression profiles. Subsequently, doublet-cell filtering and quality control were applied to the data from different sample types, resulting in four cell-gene matrices. For the most common type of renal cell carcinoma, ccRCC, PCA was performed followed by dimensionality reduction, resulting in the classification of cells into 17 distinct clusters (Fig. 1A).

The 17 cell clusters were further characterized and grouped based on the specific marker gene expression of different cell populations, which revealed seven major categories: Epithelial cells, T cells, monocytes/macrophages, endothelial cells, fibroblasts, plasmacytoid dendritic cells and mast cells (Fig. 1B). The distribution of the number of transcripts captured in each cell were visualized on the cluster plot (Fig. 1C). By examining the distribution levels of each cell population across the samples (Fig. 1D), it was observed that T cells and epithelial cells were the predominant cell populations in ccRCC, while other cell types were relatively rare. Additionally, correlation analysis among the cell populations showed that each cluster was independent and endothelial cells were the most independent stromal cell type in the tumor microenvironment, which had the lowest correlation with other cell types (Fig. 1E).

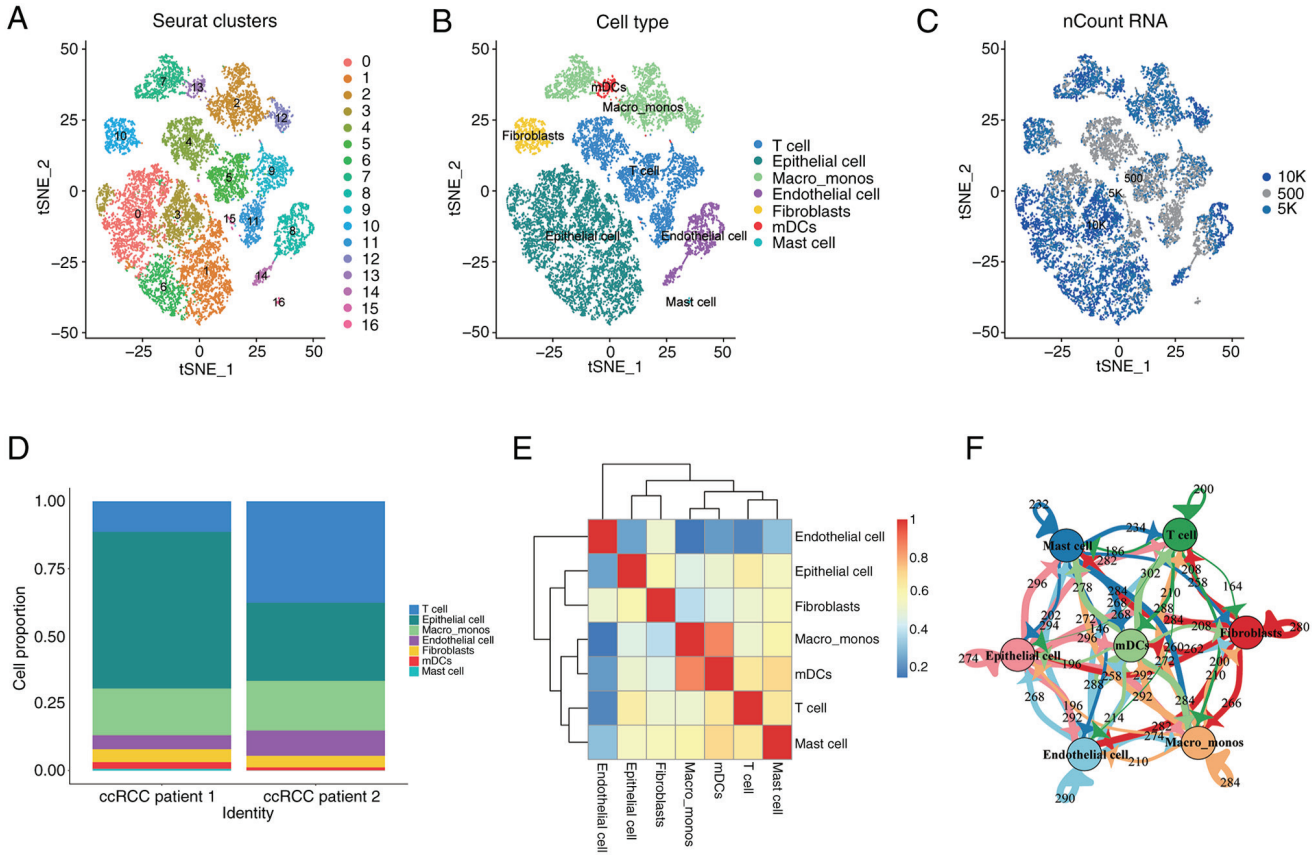

Figure 1. Overview of the single-cell mapping of data from the GSE152938 dataset. tSNE plots of (A) cell dimensionality reduction clusters, (B) cell types and (C) RNA count levels. (D) Bar plot showing the relative proportion of different cell types. (E) Correlation heatmap of the cell groups. (F) Cell communication diagram. tSNE, t-distributed stochastic neighbor embedding; mDCs, myeloid dendritic cells; macro_monos, macrophage/monocytes. ccRCC, clear cell renal cell carcinoma.

Numerous interactions and mutual influences among different cell populations were observed within the tumor microenvironment (Fig. 1E and F).

Similarly, cell clustering and visualization analysis were performed on papillary RCC, chromophobe RCC and normal kidney tissues (Fig. S1). Different types of RCC exhibited heterogeneity in the composition of their cell populations.

Malignancy and heterogeneity analysis of ccRCC epithelial cells. The epithelial cell population of ccRCC exhibits abundant heterogeneity, with a total of 6,943 epithelial cells identified by the cell identification analysis. Based on the marker gene expression patterns and predicted functional characteristics of each cell cluster, six putative subtypes of epithelial cells were identified. CNV analysis was performed on each cell cluster to identify tumor cells. Clusters C1 and C5 were found to exhibit the lowest levels of CNV, while clusters C2-4 and C6 showed higher levels of CNV (Fig. 2A). Therefore, it was initially hypothesized that the former clusters represented normal epithelial cell populations, while the latter represented tumor epithelial cell populations. Subsequently, a combination of marker gene expression and prediction using the SingleR package was used for the further identification and characterization of the epithelial cell subtypes (Fig. 2B).

GO and KEGG functional and pathway enrichment analyses were performed on the six subtypes of epithelial cells, as shown in Fig. 2C. Functional and pathway similarities were observed between the two normal cell populations, N1 and N2, while significant functional heterogeneity was observed among the cancer cell populations C1-C4. Among all subtypes, it was noted that the Ep-C4-TNF signaling cell population, which represents a small proportion of the cells, was enriched in important pathways such as 'TNF signaling pathway', 'Salmonella infection', 'Human T-cell leukemia virus 1 infection,' and 'Apoptosis'. Furthermore, its functions were significantly enriched in 'cellular response to tumor necrosis factor', 'response to tumor necrosis factor', 'post-translational protein modification' and 'response to interleukin-1'. Thus, a clear association between this cell population and TNF was identified. TNF has both beneficial and detrimental effects in tumor progression, as it has the potential to inhibit tumor cell proliferation as well as the ability to induce tumor growth (24,25). It was originally found that macrophages secrete this cytokine into the tumor microenvironment, inducing the apoptosis of tumor cells and exerting antitumor effects (26,27). However, subsequent studies discovered that tumor cells also secrete TNF, leading to cytotoxic resistance, immune escape, the promotion of cancer cell infiltration, tumor vascularization and the induction of cancer cell differentiation (28,29).

Using the PROGENy package (Fig. 2D), the classical tumor pathways that these cell populations may be involved in were investigated. It was found that the complexity of the role of each cell population in ccRCC tissue varies in different

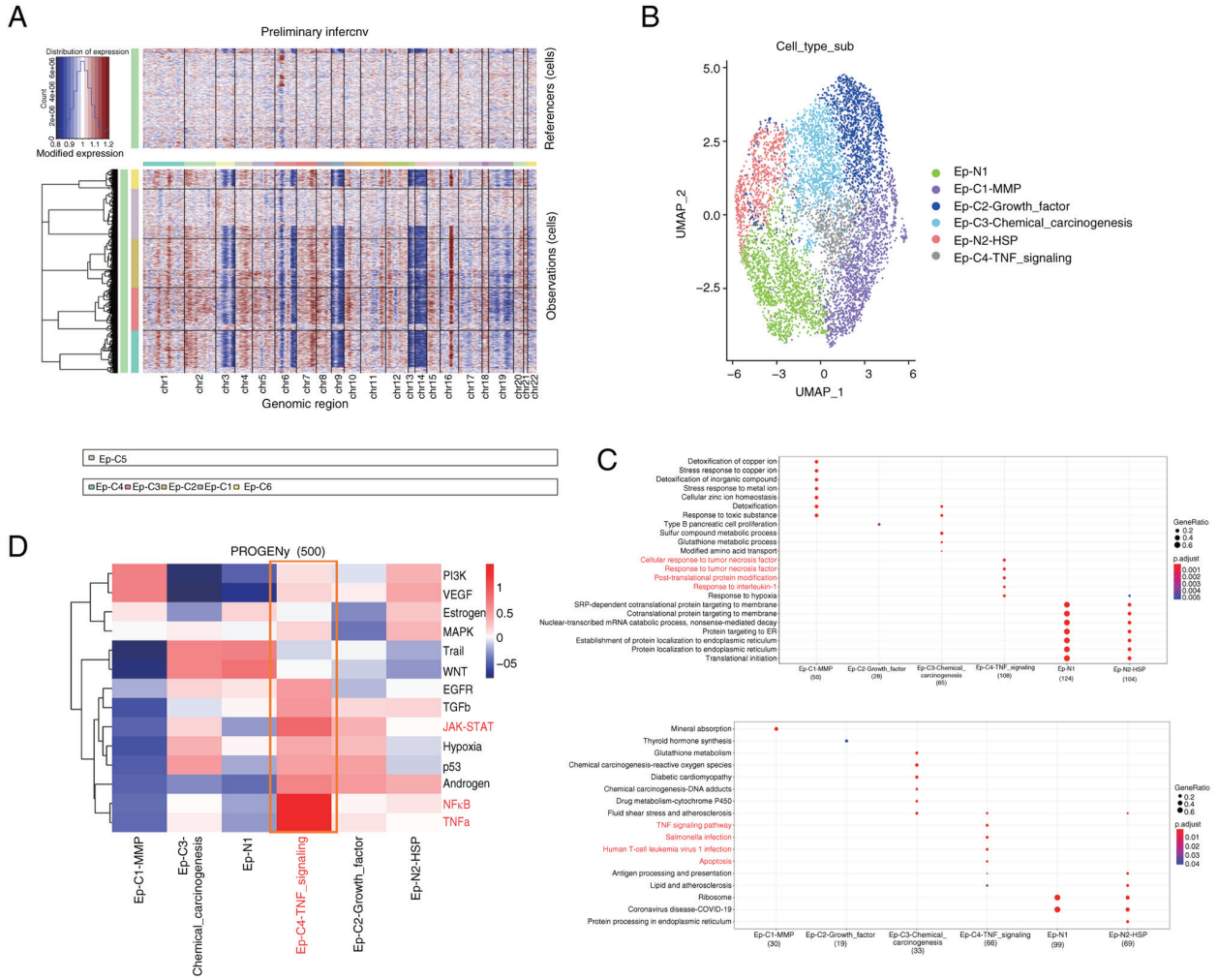

Figure 2. Epithelial cell heterogeneity and malignant in clear cell renal cell carcinoma. (A) CNV heatmap showing the diverse malignancy level of cells. (B) UMAP plot revealing the six subtypes of epithelial cells. (C) Bubble charts of Gene Ontology functional enrichment results and Kyoto Encyclopedia of Genes and Genomes pathway enrichment results for epithelial cell subsets. These indicate the significant enrichment of the Ep-C4-TNF subset in functional categories and pathways related to TNF-associated mechanisms. (D) PROGENy heatmap showing the enrichment of epithelial cell subsets in abnormal tumor-associated pathways. CNV, copy number variation; UMAP, uniform manifold approximation and projection; Ep, epithelial; p.adjust, adjusted P-value.

tumor pathways. Notably, cell population C1 was enriched in the classic PI3K/AKT tumor pathway and VEGF signaling pathway, both of which are associated with tumor angiogenesis. In addition, cell population C4 showed significant enrichment in the TNF-α and NF-κB pathways, which promote uncontrolled cell growth and tumor progression (30,31).

Subsequently, a correlation analysis of the key TNF pathway genes, TNFRSF1A and TNFRSF1B, in ccRCC tissue were performed using TCGA database (Fig. S2). The results revealed that TNFRSF1A gene expression clearly correlated with cell cytoskeleton- and cell motility-related genes, namely MAP7 domain containing 1, tubulin β 6 classV and zyxin. By contrast, TNFRSF1B gene expression closely correlated with tumor angiogenesis-related genes, namely IL16, WASP actin nucleation promoting factor and vav guanine nucleotide exchange factor 1. Moreover, the protein expression levels of these genes in the cancer cell population were markedly higher than those in the non-cancer cell population, as revealed by analysis of ccRCC data from the CPTAC database.

Based on the results of the enrichment analysis, it may be speculated that TNF-associated epithelial cell populations play a role in increasing tumor immune resistance, promoting cancer cell motility and infiltration, and facilitating tumor angiogenesis within the tumor tissue. This suggests that targeting such cell populations could serve as a therapeutic target in antitumor immune therapy.

TNF signaling networks in the complex microenvironment of ccRCC. Following exploration of the heterogeneity of epithelial cells in the ccRCC microenvironment, the immune composition and constructed networks of this microenvironment were analyzed. Based on the characteristics of cell populations and the specific expression of marker genes, three subgroups within the monocyte/macrophage cell population were identified, namely the Macro_M1, Macro_M2, and Monocyte groups (Fig. 3A). Through pseudotime analysis, it was observed that the monocyte cell population evolved into M1 and M2 macrophages at the pseudotime starting point (Fig. 3B), which is consistent with the theory that monocytes transition into macrophages (32). Furthermore, the subtyping analysis of T cells was performed (Fig. S3A) and T cells were divided into six distinct subgroups based on their characteristics. Through

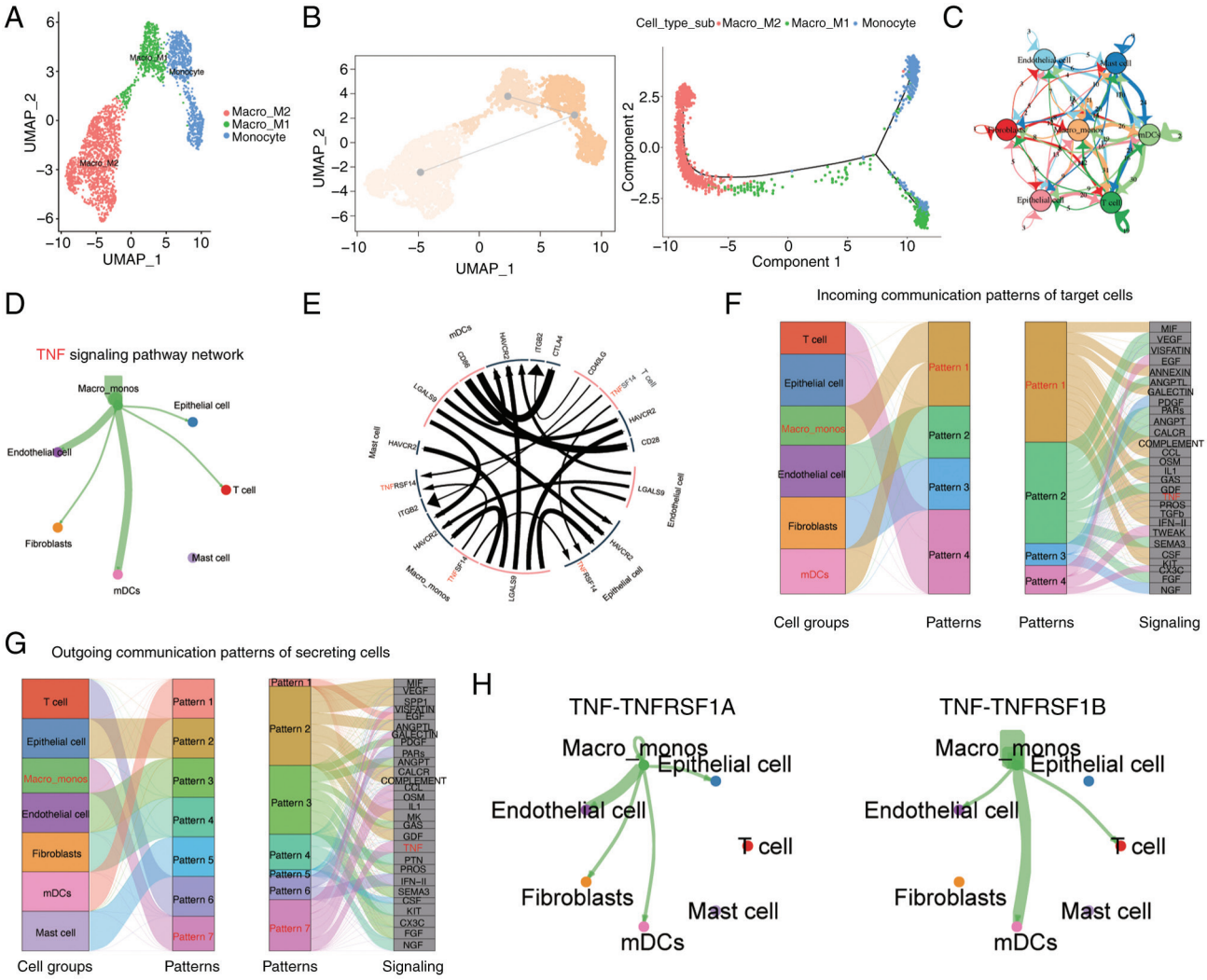

Figure 3. TNF signaling pathway features highly in the complex crosstalk network in the ccRCC tumor microenvironment. (A) UMAP plot of macro_mono cell subtypes. (B) Pseudo temporal map of macro_mono subtypes. (C) iTALK network showing that macro_mono cells were the most active in cytokine communication. (D) Network plot of the TNF signaling pathway network in ccRCC. (E) Circle plot of significant L-R pairs among all cell types in ccRCC. (F) Riverplot of key pathways in the incoming communication patterns of target cell groups. (G) Riverplot of key pathways in the outgoing communication patterns of secreting cell groups. (H) Network plot showing the main crosstalk of L-R pairs associated with the TNF signaling pathway in ccRCC. ccRCC, clear cell renal cell carcinoma; UMAP, uniform manifold approximation and projection; macro_mono, macrophage/monocyte; L-R, ligand-receptor; mDCs, myeloid dendritic cells; TNFRSF1A/B, TNF receptor superfamily member 1A/B.

functional enrichment analysis, a cluster of highly proliferative CD8+ T-cell subtypes was identified. These cells showed enrichment in GO functions associated with mitotic nuclear division, nuclear division, organelle fission and chromosome segregation (Fig. S3B). This implies that following the stimulation of ccRCC, this cell cluster is activated to undergo rapid proliferation, with an expansion in number via cell division, and an enhanced ability to combat pathogens or tumors. These highly active cells are likely to exhibit strong cytotoxic activity and eliminate abnormal cells via the release of cytotoxic substances. Therefore, the proliferative activity of this cell population may be crucial for an effective immune response.

Subsequently, to investigate the intercellular communication occurring within the ccRCC microenvironment, the CellChat method was used to construct a comprehensive cell communication network and visualize the top interacting pairs and communicating cell populations. This indicated that the monocyte/macrophage cell population exhibited a prominent presence in the microenvironmental communication network (Fig. 3C). Key pathways involved in important communication processes were predicted and the TNF signaling pathway was identified as one of the most crucial pathways (Fig. 3E-G). Through this signaling pathway analysis, it was observed that monocyte/macrophage cells were the predominant senders of signals compared with other cell types, while other cell types, with the exception of mast cells, were regulated by this signal (Fig. 3D). The major interacting pairs within this network were found to be TNF-TNFRSF1A and TNF-TNFRSF1B (Fig. 3H). TNFRSF1A, also known as TNFR1, is expressed on almost all cells in the body. By contrast, TNFRSF1B, also known as TNFR2, is considered to be highly specific to the tumor microenvironment and is a potential driver of immune escape and tumor proliferation (33,34).

To further investigate the potential role of monocyte/macrophage cells in the epithelial cancer cell population of ccRCC, the gene expression profile of ccRCC in TCGA database was

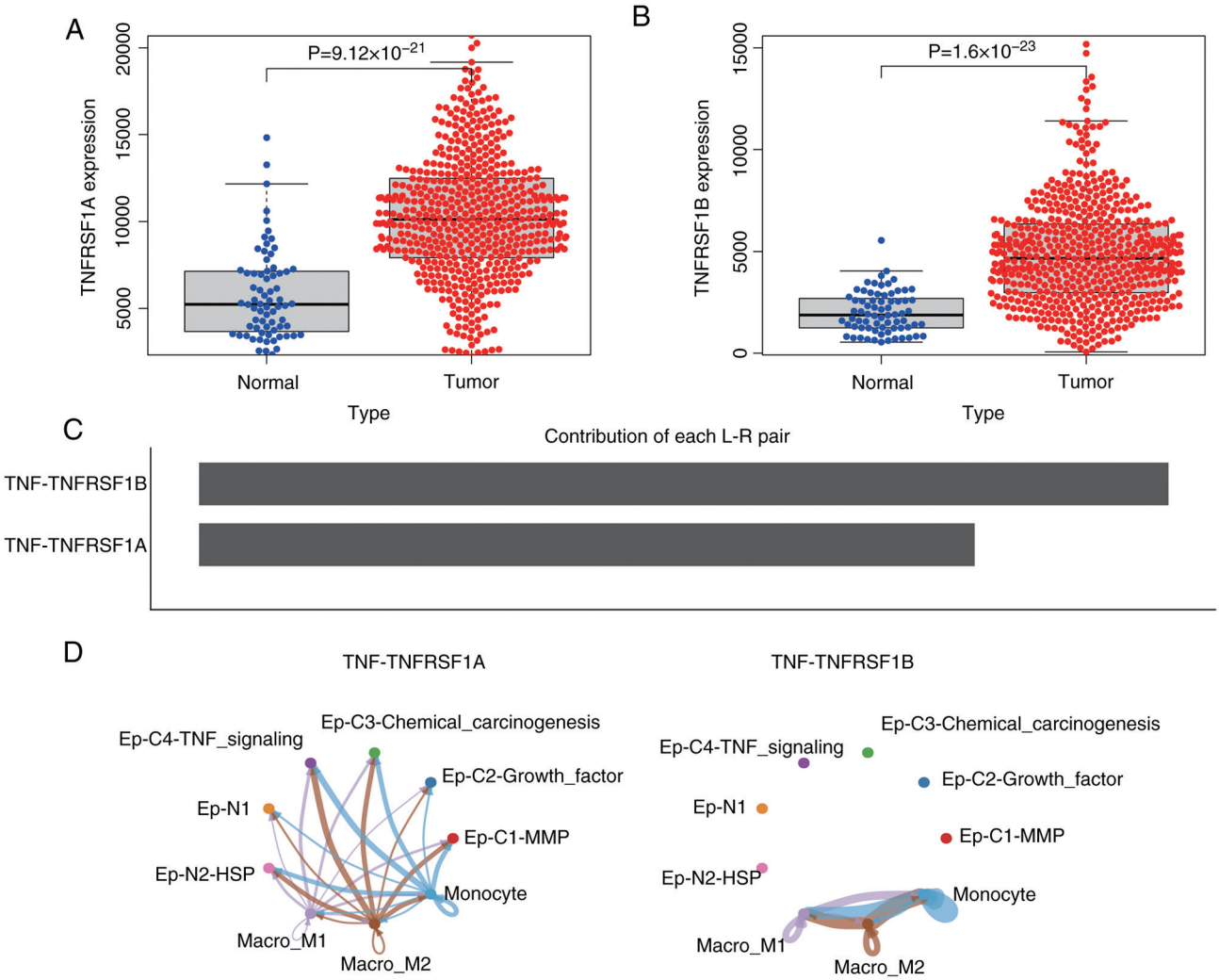

Figure 4. Comparison of TNFRSF1A and TNFRSF1B in ccRCC. Box plots show that (A) TNFRSF1A and (B) are upregulated in ccRCC tissue compared with normal tissue. (C) Relative contribution levels of the TNF-TNFRSF1A and TNF-TNFRSF1B signaling pathways. (D) Network plot showing the main crosstalk of L-R pairs between Ep and macro_mono_subtypes. TNFRSF1A/B, TNF receptor superfamily member 1A/B; ccRCC, clear cell renal cell carcinoma; L-R, ligand-receptor; Ep, epithelial; macro_mono, macrophage/monocyte.

analyzed. The results revealed that the expression levels of TNFRSF1A and TNFRSF1B in ccRCC were significantly higher than in normal tissues (Fig. 4A and B). Additionally, a communication network between monocyte/macrophage cells and epithelial cells was constructed. The results predicted that the interaction weight of TNF-TNFRSF1B was higher than that of TNFRSF1A (Fig. 4C), and the interaction with TNF-TNFRSF1B was limited to subgroups of monocyte/macrophage cells, while the TNF-TNFRSF1A network exhibited cross-talk between monocyte/macrophage cell subgroups and epithelial cell subgroups (Fig. 4D). This suggests that TNF activates various signaling pathways through TNFRSF1A, such as the NF-κB and MAPK pathways in the Ep-C4-TNF-signaling cell subgroup, thereby influencing cancer cell proliferation, survival and metastasis. However, the interaction between TNF and TNFRSF1A may directly affect other cells involved in inflammation and immune regulation, and impact the survival, proliferation and cytokine production of other epithelial and immune cells, thus affecting immune function. Furthermore, these findings suggest that the interaction between TNF and TNFRSF1B modulates the immune response in the tumor microenvironment, indirectly influencing tumor immune evasion and the effectiveness of antitumor immune therapy.

In normal kidney tissue, the TNF pathway also exhibits significant intercellular crosstalk, but this is limited to interactions between monocyte/macrophage cells and immune cells. The corresponding receptor genes were found not to be activated on the surface of normal tissue epithelial cells (Fig. S4). The TNF-TNFRSF1B interaction network in normal tissue exhibited a pronounced high-weight interaction. In comparison to the TNF pathway in ccRCC, TNF-TNFRSF1B signaling demonstrated a more pronounced intensity in cancer tissue. Furthermore, it is noteworthy that the TNF-TNFRSF1A interaction was found to be highly specific for the epithelial cells of ccRCC tissue.

TNFRSF1A promotes RCC progression. In the preceding analysis, the existence of a cancer cell subpopulation associated with the functionality of the TNF-associated signaling pathway was identified. Furthermore, in the RCC communication network, the strength and specificity of the

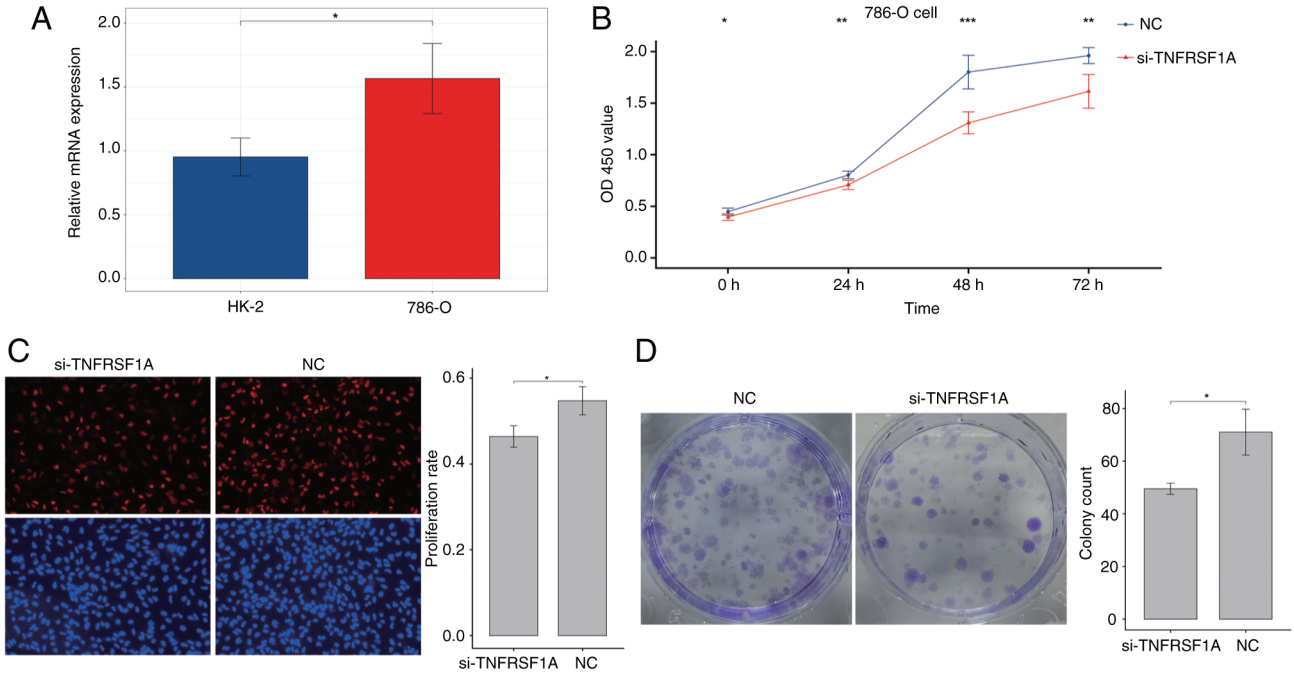

Figure 5. Knockdown of TNFRSF1A expression inhibits the proliferation of 786-O cells. (A) Bar chart showing that the expression of TNFRSF1A in the 786-O cancer cell line is upregulated compared with that in the normal HK-2 cell line. (B) Cell Counting Kit-8 assay results showed that the cell proliferation rate in the si-TNFRSF1A group was lower than that in the NC group 48 and 72 h after seeding. (C) 5'-Ethynyl-2'-deoxyuridine assay results confirm the lower proliferation of rate cells in the si-TNFRSF1A group compared with the NC group. Red staining shows the nuclei of cells with proliferative capacity, blue staining shows the total nuclei of viable cells, and the red/blue ratio indicates the proliferation rate. Magnification, x100. (D) Cells transfected with si-TNFRSF1A exhibited weaker colony formation ability compared with those transfected with si-NC. Data are presented as the mean ± SD of at least three independent experiments. *P<0.05, **P<0.01 and ***P<0.001 for si-TNFRSF1A vs. NC. TNFRSF1A, TNF receptor superfamily member 1A; si, small interfering RNA; NC, negative control transfected with si-NC; OD450, optical density at 450 nm.

TNF-TNFRSF1B interaction were higher than those in normal tissue. However, the TNF-TNFRSF1A interaction exhibited greater specificity, particularly in the communication process between monocytes/macrophages and epithelial cells in RCC. In a previous study, Hwang *et al* (35) identified the TNF signaling pathway as being pivotal in the context of tyrosine kinase inhibitor (TKI) resistance in advanced ccRCC, and suggested that TNFRSF1A expression could potentially serve as a predictive biomarker for an unfavorable clinical response to TKIs in ccRCC. Therefore, the present study focused on the specific perturbation of TNFRSF1A in the epithelial cell population.

Firstly, the expression of TNFRSF1A was tested in the renal cancer cell line 786-O and the normal renal cell line HK-2 via RT-qPCR (Fig. 5A). The results showed that TNFRSF1A expression in the tumor cell line was significantly higher compared with that in the normal cell line. Then, the expression of TNFRSF1A was knocked down in 786-O cells using siRNA (Fig. S5) and the transfected cells were analyzed in a CCK-8 experiment. The results showed a significant reduction the proliferation of the renal cancer cells transfected with si-TNFRSF1A compared with those transfected with si-NC (Fig. 5B). Additionally, cell proliferation was further examined using the EdU assay and a significant reduction in the proliferation rate in the experimental group was observed following TNFRSF1A knockdown compared with that in the NC group (Fig. 5C). Furthermore, the results of the colony formation assay using the treatment and control renal cancer cells showed that colony formation in the si-TNFRSF1A group was significantly lower than that in the NC group, indicating a significant reduction in independent survival capability (Fig. 5D). Therefore, it was concluded that TNFRSF1A promotes ccRCC cell proliferation.

Subsequently, a wound healing assay and Transwell migration and invasion assays were conducted to further investigate the effects of TNFRSF1A knockdown, The results demonstrated that cell migration in the treatment group was significantly lower than that in the NC group (Fig. 6A and B). Additionally, in the Transwell invasion assay the knockdown of TNFRSF1A significantly inhibited invasion compared with that in the NC group (Fig. 6C). These results indicate that reducing the expression of the TNFRSF1A gene negatively regulates the migration and invasion capabilities of ccRCC cells.

In addition, to further characterize the role of TNFRSF1A in renal cancer cells, flow cytometry assays were conducted to assess the cell cycle and apoptosis status of the si-TNFRSF1A and NC groups (Fig. 6D and E) The results of the cell cycle assay revealed that following TNFRSF1A knockdown the number of ccRCC cells entering the S phase from the G_0/G_1 phase significantly decreased. This suggests that elevated TNFRSF1A expression leads to an increased number of renal cancer cells entering the S phase with active DNA synthesis. Correspondingly, the results of the apoptosis assay showed that the apoptosis rate in the TNFRSF1A knockdown was significantly higher compared with that in the NC group, indicating that high TNFRSF1A expression suppresses apoptosis in ccRCC cells. Also, analysis of the variation of TNFSF1A

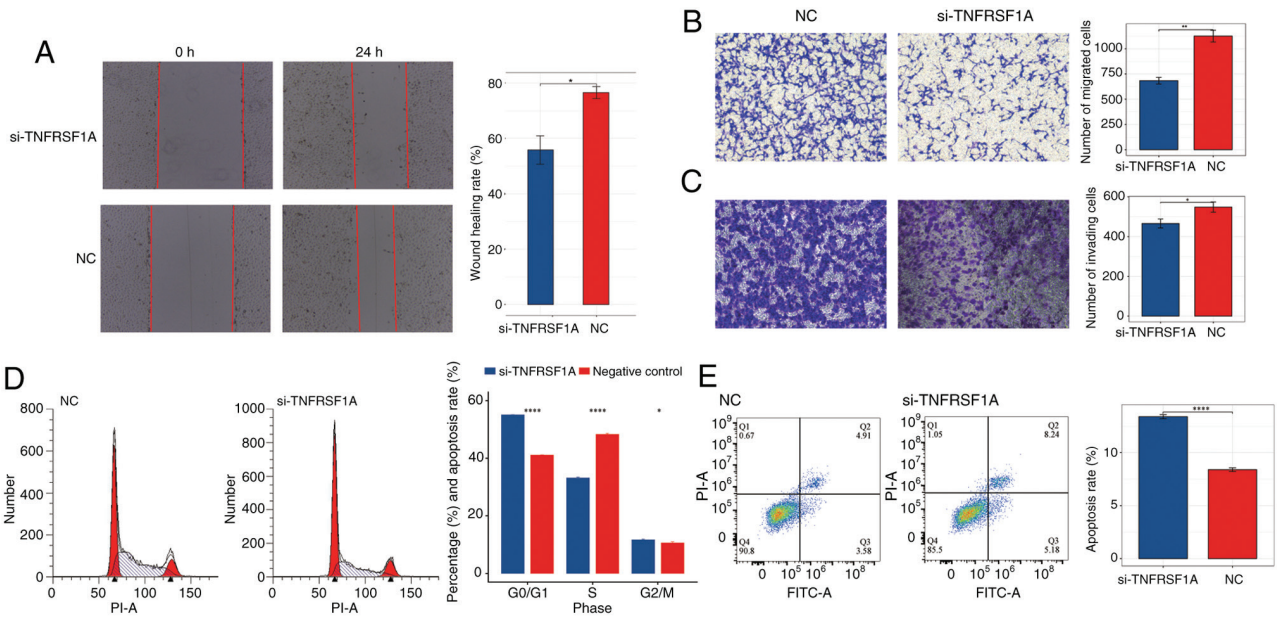

Figure 6. Role of TNFRSF1A as a promotor of clear cell renal cell carcinoma. (A) si-TNFRSF1A interference slowed down the healing of 786-O cells. Migration was quantified based on the closure of the scratch from 0 to 24 h. Magnification, x40. Transwell (B) migration and (C) invasion assays showed weaker migratory capability and reduced invasive capacity of the si-TNFRSF1A group compared with the NC group. Magnification, x100. (D) Cell cycle distribution and (E) apoptosis of the 786-O cells were detected using flow cytometry. Data are presented as the mean ± SD of at least three independent experiments. *P<0.05, **P<0.01 and ****P<0.0001 for si-TNFRSF1A vs. NC. TNFRSF1A, TNF receptor superfamily member 1A; si, small interfering RNA; NC, negative control transfected with si-NC.

expression with different clinical factors using one-way ANOVA showed that TNFRSF1A mRNA expression significantly differs according to the grade and distant metastasis of ccRCC (Table SI). Furthermore, post hoc analysis revealed a significant difference between G2 and G4 stage patients. In addition, uni- and multi-variate logistic regression analyses revealed that TNFRSF1A serves as an independent risk factor in the assessment of survival prognosis (Tables SII and SIII).

Discussion

The comprehensive analysis of the single-cell landscapes and phenotypes of RCC in the present study provides valuable insights into the cellular composition, heterogeneity and potential interactions within the tumor microenvironment. The findings shed light on the specific characteristics of ccRCC and its associated epithelial cell populations, as well as the role of TNF signaling in RCC progression.

In the analysis of ccRCC, seven distinct cell types were identified through PCA and dimensionality reduction. These clusters represent different cell types within the tumor, including epithelial cells, T cells, monocytes/macrophages, endothelial cells, fibroblasts, myeloid dendritic cells and mast cells. ccRCC itself is highly heterogeneous, and differences in the tumor microenvironment among different patients, as well as in the extent of tumor tissue resection between patient samples, can lead to differences in cell composition (36,37). The present study revealed that one sample was predominantly composed of epithelial cells, while another was predominantly composed of T cells. The predominance of T cells and epithelial cells in ccRCC suggests their potential importance in tumor development and progression. In studies on the anti-PD-1 immunotherapy of multiple patients with ccRCC, it has been consistently verified that T-cell immune infiltration is significantly associated with tumor sensitivity, PD-1 blockade response and resistance (38,39). The relatively lower abundance of other cell types indicates that their contributions to the tumor microenvironment are comparatively minor. In the present study, further characterization of the epithelial cell population in ccRCC revealed significant heterogeneity; six putative subtypes were identified. CNV analysis distinguished clusters representing normal epithelial cells from those representing tumor epithelial cells. Functional enrichment analysis demonstrated distinct functional profiles for normal epithelial cells and cancerous subtypes, highlighting the heterogeneity within the tumor epithelial cell population. Notably, the Ep-C4-TNF cell population exhibited enrichment in the TNF signaling pathway and associated pathways, indicating its potential involvement in tumor immune resistance, cancer cell motility and tumor angiogenesis. The TNF family comprises extremely versatile cytokines that play pivotal roles in the maintenance of immune homeostasis, triggering inflammation and supporting the host defense (40). Depending on the cellular context, these cytokines are able to elicit a wide range of effects, including apoptosis, necrosis, angiogenesis, activation of immune cells, differentiation and cell migration (41,42).

The association between TNF signaling and ccRCC was extensively explored in the present study. Analysis of two key genes in the TNF pathway, namely TNFRSF1A and TNFRSF1B, revealed their significant correlations with genes associated with the cell cytoskeleton, cell motility and tumor angiogenesis. The expression levels of TNFRSF1A and TNFRSF1B were also found to be higher in tumor tissues compared with those in normal tissues. Moreover, communication network analysis demonstrated the important role of TNF signaling in intercellular communication within the tumor

microenvironment, with monocytes/macrophages acting as primary signal senders. The interaction between TNF and its receptors, particularly TNFRSF1A and TNFRSF1B, was indicated to influence various cellular processes, including cancer cell proliferation, survival, metastasis and immune responses. These findings have important implications in understanding the complex microenvironment of ccRCC and the potential therapeutic implications. In other types of tumors, the interaction between monocyte-derived TNF-α and tumor cell TNFRSF1B has been shown to trigger the occurrence of tumorigenic inflammation (43). This signaling pathway also serves as a crucial regulatory factor in the immune-suppressive function of endothelial progenitor cells (44). Therefore, targeting TNF-associated epithelial cell populations and the TNF signaling pathway may provide new opportunities for antitumor immune therapy. The heterogeneity observed within the epithelial cell population also highlights the requirement for a personalized approach in cancer treatment. Additionally, the characterization of the immune cell composition and communication networks provides valuable insights into the immune response and potential immunotherapeutic targets in RCC.

Although the TNF signaling pathway has garnered extensive research attention in the field of cancer, further exploration of its role in ccRCC is imperative. The various members of the TNF family exhibit heterogeneity in their functions (45,46). In the present study, during the identification process of distinct subpopulations within the epithelial cell cluster, a subset of cancer cells enriched with functions relevant to TNF-associated signaling pathways was discovered. Furthermore, while the intensity and specificity of TNF-TNFRSF1B interactions in the RCC communication network were found to be higher than those in normal tissues, it is noteworthy that the interactions of TNF-TNFRSF1A exhibited greater specificity, particularly in the communication between monocyte/macrophage cells and epithelial cells in RCC. The key proteins associated with positively correlated receptor genes and the potential mechanisms of carcinogenesis were also explored.

TNFRSF1A and TNFRSF1B are the most well-characterized members of the TNFR superfamily (47). TNFRSF1B is preferentially expressed in leukocytes, while TNFRSF1A is reported to be expressed in most cell types (48,49). Nevertheless, the present study indicated that the interactions of TNF-TNFRSF1A exhibited greater specificity than those of TNF-TNFRSF1B within renal cancer tissues. Thus, cell biology experiments were performed to further validate the oncogenic role of the receptor gene TNFRSF1A. The knockdown of TNFRSF1A expression reduced RCC cell proliferation, indicating that the upregulated expression of TNFRSF1A promotes the proliferation of RCC. Similarly, the results of *in vitro* experiments indicated that TNFRSF1A promotes RCC cell migration and invasion. Moreover, the knockdown of TNFRSF1A was shown to promote apoptosis and reduce cell cycle progression, indicating that this receptor gene inhibits apoptosis when highly expressed, and significantly facilitates the entry of cancer cells to the S-phase for DNA replication. These experimental findings collectively demonstrate the specific functions of TNFRSF1A as a driver of tumor progression in RCC cells. These results provide valuable insights for the selection of suitable targeted treatment strategies in clinical practice and lay the foundation for the exploration of other potential therapeutic targets.

However, the study has certain limitations. For example, in the analysis of clinical samples, the collection and measurement of TNFRSF1A expression in primary kidney cancer tissue samples from patients were not performed. Instead, data from TCGA database was used to analyze the expression of TNFRSF1A and its clinical associations in ccRCC. Although TCGA data is extensive, the uniformity in sample processing and analysis methods might introduce biases. The direct measurement of TNFRSF1A expression in patient samples would more accurately reflect individual differences and provide a deeper understanding of the specific biological role of TNFRSF1A in kidney cancer. In addition, the effectiveness of TNFRSF1A as a potential therapeutic target was not validated. The following experimental strategies are suggested to investigate the targeting of TNFRSF1A in ccRCC: Firstly, identify TNFRSF1A-specific inhibitors and optimize their structures. Secondly, conduct validation experiments *in vitro* to evaluate the impact of the inhibitors on tumor growth, cell apoptosis and other biomarkers. Lastly, perform *in vivo* experiments using animals to assess the safety and potential side effects of the TNFRSF1A inhibitors. This may address the limitations of the present study.

In summary, a comprehensive analysis of the single-cell landscape and phenotypes of RCC was conducted in the present study, which highlighted the heterogeneity within the tumor microenvironment and the potential role of the TNF signaling pathway in RCC progression. The specificity and pro-cancer effects of TNFRSF1A in renal cancer were further validated through *in vitro* experiments. These findings contribute to an improved understanding of RCC biology, and may guide future research and therapeutic strategies.

Acknowledgements

Not applicable.

Funding

The study was supported by a grant from the Project of NINGBO Leading Medical & Health Discipline (project no. 2022-X11).

Availability of data and materials

The data generated in the present study may be found in the TCGA database at the following URL: https://portal.gdc.cancer.gov, and in the Gene Expression Omnibus database under accession number GSE152938 or at the following URL: https://www.ncbi.nlm.nih.gov/geo/query/acc.cgi?acc=GSE152938. The other data generated in the present study may be requested from the corresponding author.

Authors' contributions

LY and ZD conceived the study. LY and JZ performed the bioinformatics analyziz. LY, ZD and PX performed the experiments, and ZD and JZ provided scientific advice. XX and JZ performed data analysis of the cell experiments. LY wrote the manuscript and XX revised the manuscript. LY and JZ

confirm the authenticity of all the raw data. All authors read and approved the final version of the manuscript.

Ethics approval and consent to participate

Not applicable.

Patient consent for publication

Not applicable.

Competing interests

The authors declare that they have no competing interests.

References

1. Capitanio U, Bensalah K, Bex A, Boorjian SA, Bray F, Coleman J, Gore JL, Sun M, Wood C and Russo P: Epidemiology of renal cell carcinoma. Eur Urol 75: 74-84, 2019.
2. Cirillo L, Innocenti S and Becherucci F: Global epidemiology of kidney cancer. Nephrol Dial Transplant 39: 920-928, 2024.
3. Choueiri TK: Renal cell carcinoma. Hematol Oncol Clin North Am 25: xiii-xiv, 2011.
4. Diaz-Montero CM, Rini BI and Finke JH: The immunology of renal cell carcinoma. Nat Rev Nephrol 16: 721-735, 2020.
5. Chowdhury N and Drake CG: Kidney cancer: An overview of current therapeutic approaches. Urol Clin North Am 47: 419-431, 2020.
6. Bahadoram S, Davoodi M, Hassanzadeh S, Bahadoram M, Barahman M and Mafakher L: Renal cell carcinoma: An overview of the epidemiology, diagnosis, and treatment. G Ital Nefrol 39: 2022-vol3, 2022.
7. Gray RE and Harris GT: Renal cell carcinoma: Diagnosis and management. Am Fam Physician 99: 179-184, 2019.
8. Hancock SB and Georgiades CS: Kidney cancer. Cancer J 22: 387-392, 2016.
9. Li F, Aljahdali IAM, Zhang R, Nastiuk KL, Krolewski JJ and Ling X: Kidney cancer biomarkers and targets for therapeutics: Survivin (BIRC5), XIAP, MCL-1, HIF1alpha, HIF2alpha, NRF2, MDM2, MDM4, p53, KRAS and AKT in renal cell carcinoma. J Exp Clin Cancer Res 40: 254, 2021.
10. Sharma R, Kadife E, Myers M, Kannourakis G, Prithviraj P and Ahmed N: Determinants of resistance to VEGF-TKI and immune checkpoint inhibitors in metastatic renal cell carcinoma. J Exp Clin Cancer Res 40: 186, 2021.
11. Tonooka A and Ohashi R: Current trends in anti-cancer molecular targeted therapies: Renal complications and their histological features. J Nippon Med Sch 89: 128-138, 2022.
12. Miao D, Margolis CA, Gao W, Voss MH, Li W, Martini DJ, Norton C, Bossé D, Wankowicz SM, Cullen D, *et al*: Genomic correlates of response to immune checkpoint therapies in clear cell renal cell carcinoma. Science 359: 801-806, 2018.
13. Topalian SL, Taube JM, Anders RA and Pardoll DM: Mechanism-driven biomarkers to guide immune checkpoint blockade in cancer therapy. Nat Rev Cancer 16: 275-287, 2016.
14. Fischer R, Kontermann RE and Pfizenmaier K: Selective targeting of TNF receptors as a novel therapeutic approach. Front Cell Dev Biol 8: 401, 2020.
15. Liu W, Yan B, Yu H, Ren J, Peng M, Zhu L, Wang Y, Jin X and Yi L: OTUD1 stabilizes PTEN to inhibit the PI3K/AKT and TNF-alpha/NF-kappaB signaling pathways and sensitize ccRCC to TKIs. Int J Biol Sci 18: 1401-1414, 2022.
16. Richter F, Williams SK, John K, Huber C, Vaslin C, Zanker H, Fairless R, Pichi K, Marhenke S, Vogel A, *et al*: The TNFR1 antagonist atrosimab is therapeutic in mouse models of acute and chronic inflammation. Front Immunol 12: 705485, 2021.
17. Su C, Lv Y, Lu W, Yu Z, Ye Y, Guo B, Liu D, Yan H, Li T, Zhang Q, *et al*: Single-Cell RNA sequencing in multiple pathologic types of renal cell carcinoma revealed novel potential tumor-specific markers. Front Oncol 11: 719564, 2021.
18. Liu J, Fan Z, Zhao W and Zhou X: Machine intelligence in single-cell data analysis: Advances and new challenges. Front Genet 12: 655536, 2021.
19. Street K, Risso D, Fletcher RB, Das D, Ngai J, Yosef N, Purdom E and Dudoit S: Slingshot: Cell lineage and pseudotime inference for single-cell transcriptomics. BMC Genomics 19: 477, 2018.
20. Armingol E, Officer A, Harismendy O and Lewis NE: Deciphering cell-cell interactions and communication from gene expression. Nat Rev Genet 22: 71-88, 2021.
21. Jin S, Guerrero-Juarez CF, Zhang L, Chang I, Ramos R, Kuan CH, Myung P, Plikus MV and Nie Q: Inference and analysis of cell-cell communication using CellChat. Nat Commun 12: 1088, 2021.
22. Chandrashekar DS, Karthikeyan SK, Korla PK, Patel H, Shovon AR, Athar M, Netto GJ, Qin ZS, Kumar S, Manne U, *et al*: UALCAN: An update to the integrated cancer data analysis platform. Neoplasia 25: 18-27, 2022.
23. Livak KJ and Schmittgen TD: Analysis of relative gene expression data using real-time quantitative PCR and the 2(-Delta Delta C(T)) method. Methods 25: 402-408, 2001
24. Balkwill F: Tumour necrosis factor and cancer. Nat Rev Cancer 9: 361-371, 2009.
25. Saha P and Smith A: TNF-α (Tumor Necrosis Factor-α). Arterioscler Thromb Vasc Biol 38: 2542-2543, 2018.
26. Eisenman ST, Gibbons SJ, Verhulst PJ, Cipriani G, Saur D and Farrugia G: Tumor necrosis factor alpha derived from classically activated 'M1' macrophages reduces interstitial cell of Cajal numbers. Neurogastroenterol Motil 29: 10.1111, 2017.
27. Shapouri-Moghaddam A, Mohammadian S, Vazini H, Taghadosi M, Esmaeili SA, Mardani F, Seifi B, Mohammadi A, Afshari JT and Sahebkar A: Macrophage plasticity, polarization, and function in health and disease. J Cell Physiol 233: 6425-6440, 2018.
28. Garancher A, Suzuki H, Haricharan S, Chau LQ, Masihi MB, Rusert JM, Norris PS, Carrette F, Romero MM, Morrissy SA, *et al*: Tumor necrosis factor overcomes immune evasion in p53-mutant medulloblastoma. Nat Neurosci 23: 842-853, 2020.
29. Masola V, Greco N, Tozzo P, Caenazzo L and Onisto M: The role of SPATA2 in TNF signaling, cancer, and spermatogenesis. Cell Death Dis 13: 977, 2022.
30. Yu H, Lin L, Zhang Z, Zhang H and Hu H: Targeting NF-κB pathway for the therapy of diseases: Mechanism and clinical study. Signal Transduct Target Ther 5: 209, 2020.
31. Balkwill F: TNF-alpha in promotion and progression of cancer. Cancer Metastasis Rev 25: 409-416, 2006.
32. Tacke F and Zimmermann HW: Macrophage heterogeneity in liver injury and fibrosis. J Hepatol 60: 1090-1096, 2014.
33. Takahashi H, Yoshimatsu G and Faustman DL: The roles of TNFR2 signaling in cancer cells and the tumor microenvironment and the potency of TNFR2 targeted therapy. Cells 11: 1952, 2022.
34. Speeckaert MM, Speeckaert R, Laute M, Vanholder R and Delanghe JR: Tumor necrosis factor receptors: Biology and therapeutic potential in kidney diseases. Am J Nephrol 36: 261-270, 2012.
35. Hwang HS, Park YY, Shin SJ, Go H, Park JM, Yoon SY, Lee JL and Cho YM: Involvement of the TNF-α pathway in TKI resistance and suggestion of TNFR1 as a predictive biomarker for TKI responsiveness in clear cell renal cell carcinoma. J Korean Med Sci 35: e31, 2020.
36. Dong B, Miao J, Wang Y, Luo W, Ji Z, Lai H, Zhang M, Cheng X, Wang J, Fang Y, *et al*: Single-cell analysis supports a luminal-neuroendocrine transdifferentiation in human prostate cancer. Commun Biol 3: 778, 2020.
37. Couturier CP, Ayyadhury S, Le PU, Nadaf J, Monlong J, Riva G, Allache R, Baig S, Yan X, Bourgey M, *et al*: Single-cell RNA-seq reveals that glioblastoma recapitulates a normal neurodevelopmental hierarchy. Nat Commun 11: 3406, 2020.
38. Braun DA, Hou Y, Bakouny Z, Ficial M, Angelo MS, Forman J, Ross-Macdonald P, Berger AC, Jegede OA, Elagina L, *et al*: Interplay of somatic alterations and immune infiltration modulates response to PD-1 blockade in advanced clear cell renal cell carcinoma. Nat Med 26: 909-918, 2020.
39. Au L, Hatipoglu E, de Massy M, Litchfield K, Beattie G, Rowan A, Schnidrig D, Thompson R, Byrne F, Horswell S, *et al*: Determinants of anti-PD-1 response and resistance in clear cell renal cell carcinoma. Cancer Cell 39: 1497-1518 e1411, 2021.
40. Wajant H: The role of TNF in cancer. Results Probl Cell Differ 49: 1-15, 2009.
41. Gao M, Li X, Yang M, Feng W, Lin Y and He T: TNFAIP3 mediates FGFR1 activation-induced breast cancer angiogenesis by promoting VEGFA expression and secretion. Clin Transl Oncol 24: 2453-2465, 2022.

42. Messeha SS, Zarmouh NO, Antonie L and Soliman KFA: Sanguinarine inhibition of TNF-α-induced CCL2, IKBKE/NF-κB/ERK1/2 signaling pathway, and cell migration in human triple-negative breast cancer cells. Int J Mol Sci 23: 8329, 2022.
43. Tomolonis JA, Xu X, Dholakia KH, Zhang C, Guo L, Courtney AN, Wang S, Balzeau J, Barragán GA, Tian G, *et al*: Interaction between tumor cell TNFR2 and monocyte membrane-bound TNF-α triggers tumorigenic inflammation in neuroblastoma. J Immunother Cancer 11: e005478, 2023.
44. Naserian S, Abdelgawad ME, Bakshloo MA, Ha G, Arouche N, Cohen JL, Salomon BL and Uzan G: The TNF/TNFR2 signaling pathway is a key regulatory factor in endothelial progenitor cell immunosuppressive effect. Cell Commun Signal 18: 94, 2020.
45. Siegmund D, Wagner J and Wajant H: TNF receptor associated factor 2 (TRAF2) signaling in cancer. Cancers (Basel) 14: 4055, 2022.
46. Hira K and Begum AS: Methods for evaluation of TNF-α inhibition effect. Methods Mol Biol 2248: 271-279, 2021.
47. Xing-Rong W, Sheng-Qian X, Wen L, Shan Q, Fa-Ming P and Jian-Hua X: Role of TNFRSF1A and TNFRSF1B polymorphisms in susceptibility, severity, and therapeutic efficacy of etanercept in human leukocyte antigen-B27-positive Chinese Han patients with ankylosing spondylitis. Medicine (Baltimore) 97: e11677, 2018.
48. Shi G and Hu Y: TNFR1 and TNFR2, which link NF-κB activation, drive lung cancer progression, cell dedifferentiation, and metastasis. Cancers (Basel) 15: 4299, 2023.
49. Miller PG, Bonn MB and McKarns SC: Transmembrane TNF-TNFR2 impairs Th17 differentiation by promoting Il2 expression. J Immunol 195: 2633-2647, 2015.